ISSN 2004-2965 Energy Proceedings, Vol. 21, 2021

International Conference on Applied Energy 2021
Nov. 29 - Dec. 5, 2021, Thailand/Virtual
Paper ID: 058

Molecular Dynamics Simulation of Methane Hydrate Growth in Water-Waxy Oil System

Qingyun Liao[1], Bohui Shi[1*], Shangfei Song[1], Xu Duan[1], Junao Wang[2], Haiyuan Yao[2], Ziyuan Feng[1], Jing Gong[1]

1 State Key Laboratory of Natural Gas Hydrate/ National Engineering Laboratory for Pipeline Safety/ MOE Key Laboratory of Petroleum Engineering/ Beijing Key Laboratory of Urban Oil and Gas Distribution Technology, China University of Petroleum-Beijing, Beijing 102249, CHINA

2 Key Lab of Deepwater Engineering, CNOOC Research Institute, Beijing 100028, CHINA

ABSTRACT

For the efficient exploitation of deep-water oil and gas resources, the microscopic mechanism of gas hydrate growth in the presence of waxy oil needs to be studied urgently. This work applied molecular dynamics (MD) simulations to explore the effect of wax molecules on methane hydrate growth. Based on the analysis of crystal growth, wax crystallization, and potential energy, the simulation results indicated that the addition of non-surface-active wax molecules inhibits hydrate growth, while the addition of surface-active wax molecules could extend the growth time of hydrate, thereby achieving more hydrate formation.

Keywords: methane hydrate, waxy oil, formation kinetics, wax crystallization, molecular dynamics simulation

NONMENCLATURE

Abbreviations	
MD	molecular dynamics
Symbols	
C_{18}	methyl heptadecanoate molecules
C_{17}	C_{17} normal alkane wax molecules

1. INTRODUCTION

With the proposal of China's deep-water energy strategy and the South China Sea oil and gas development strategy, the exploitation of deep-water oil and gas resources gradually deepens. For the complex three-phase flow in the production pipeline, hydrate formation and wax precipitation may occur simultaneously under the high pressure and low temperature environment, posing a threat to the safe and efficient development of oil and gas resources[1]. Therefore, research on the formation behavior of methane hydrate in water-waxy oil system has important implications on the process of deep-water oil and gas resources transportation. It is also helpful to understand hydrate formation process in the complex multiphase system, providing insights into the natural gas hydrate mining process.

The synergistic effect of hydrate formation and wax precipitation has been studied in macroscopic experiments extensively. Most studies have shown that the presence of wax crystals can inhibit the nucleation of hydrate, prolonging hydrate induction time[2–5]. However, there's no consistent conclusion on the effect of wax on hydrate growth. Some[6,7] indicated that the final amount of hydrate formed in the oil-based wax-containing system is significantly greater than that in the wax-free system, while others[8] obtained opposite conclusions.

There are few reports on the use of MD to study the growth of methane hydrate in a multiphase system containing an oil phase. Through MD carried out in gas-oil system containing water, Zi et al.[9] demonstrated the inhibition effect of asphaltene molecules on methane hydrate growth. Besides, our previous work[10] indicated that the crystallization of wax plays an important role in hydrate growth process in gas-water system. However, the effect of waxy oil on hydrate growth is not clear yet.

Therefore, based on the analysis of hydrate growth process, wax crystallization process and potential energy changes, the effect of wax molecules on hydrate growth was studied at molecular level.

Selection and peer-review under responsibility of the scientific committee of the 13th Int. Conf. on Applied Energy (ICAE2021).

2. SIMULATION DETAILS

A three-phase model, as shown in Figure 1, consists of a solid hydrate phase, a liquid water phase, and a liquid oil phase with methane dissolved. In order to investigate the effect of wax molecules on hydrate growth, methyl heptadecanoate molecules (C_{18}) or C_{17} normal alkane wax molecules (C_{17}) were dissolved randomly in the oil phase, where the C_{18}s can also act as surfactants[11]. Hence, four simulation models were built, including a pure model without any wax molecules, a 20-C_{17} model with 20 C_{17}s, a 20-C_{18} model with 20 C_{18}s, and a C_{17}-C_{18} model with 20 C_{17}s and 20 C_{18}s.

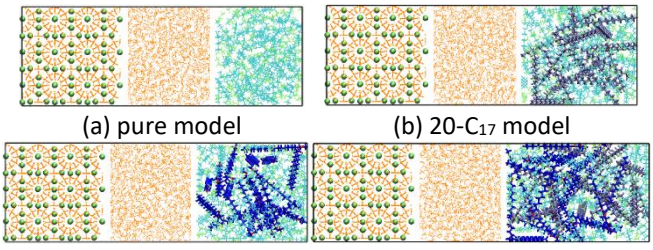

(a) pure model (b) 20-C_{17} model

(c) 20-C_{18} model (d) C_{17}-C_{18} model

Fig. 1. Initial configuration of four simulation models (orange, hydrogen bonds and water molecules; green, methane molecules; cyan, heptane molecules; iceblue, C_{17}s; blue, carbon atoms and hydrogen atoms of C_{18}s; red, oxygen atoms of C_{18}s)

The TIP4P-Ew[12] and OPLS-AA[13] force fields are chosen to describe water molecules and hydrocarbon molecules in the simulations, respectively. For the L-J parameters between different types of atoms, the geometric combination rule is adopted, except that σ = 3.032 Å and ε = 0.255 kcal/mol, fitted by Cao et al[14], was used to describe the intermolecular interaction between the oxygen atoms of water molecules and the carbon atoms of methane molecules. The short-range interactions are calculated with a cutoff of 9.5 Å for L-J potential energy and 8.5 Å for the real part Coulomb energy calculation, with the long-range Coulomb energy calculated by PPPM[15]. Such a setting of force fields can efficiently reproduce the experimental hydrate phase equilibrium conditions[16].

The simulations are all carried out using LAMMPS, including energy minimization, relaxation under NVT and NPT ensemble, as well as production run under NPT ensemble. Nose-Hoover temperature thermostat with a relaxation time of 0.2 ps was used to maintain the simulation temperature of 275 K. Meanwhile, Nose-Hoover pressure thermostat with a relaxation time of 2 ps was used to maintain the simulation pressure of 50 MPa. Periodic boundary conditions were applied in all three directions. The integration timestep is set as 2 fs, considering that SHAKE algorithm[17] was used to constrain the water molecules, CH_2 groups, and CH_3 groups. The end of the simulation is set as the time when potential energy fluctuates around the equilibrium value for about 100 ns. To ensure the credibility of simulation results, three independent repeated simulations were performed for each simulation model, each with different initial velocity distributions.

3. RESULTS AND DISCUSSION

3.1 Crystal growth analysis

The typical snapshots of the four simulation models are shown in the Figure 2 to Figure 5, using the same coloring method as Figure 1. For pure model, 20-C_{17} model and 20-C_{18} model, since the three repeated simulations show similar trends, the first simulation is presented as a demonstration, respectively. For C_{17}-C_{18} model, the third simulation deviates from the other two. Hence, Figure 5.a-c are taken from the first run and Figure 5.d is from the third run to show the difference.

For pure model and 20-C_{17} model, there's still a thin water film at the left oil-hydrate interface after bulk hydrate formation and maintained for 100 ns (Figure 2 & Figure 3), which may be ascribed to the mismatch of oil-hydrate interface. On the contrary, the thin water film can be further transformed into hydrate in 20-C_{18} model and C_{17}-C_{18} model (Figure 4.b-c & Figure 5.c-d). These phenomena demonstrated that the presence of wax molecules with ester groups can change the nature of the oil-water interface, acting as surfactants and promoting hydrate formation.

In the third simulation of C_{17}-C_{18} model, dissociation of hydrate was observed at the right oil-hydrate interface after the thin water film at the left oil-hydrate interface has been transformed into hydrate (Figure 5.d). Compared to the 20-C_{18} model, the oil phase volume in C_{17}-C_{18} model increases significantly due to the increase in the number of wax molecules. Therefore, for 20-C_{18} model, the hydrophilic ends of C_{18}s, shown as red dots in Figure 4.b-c, could distribute at both ends of the oil-hydrate interface after wax crystallization, forming hydrogen bonds with water molecules and stabilizing the interfaces. For C_{17}-C_{18} model, the hydrophilic ends of C_{18} molecules mostly distribute at the left oil-hydrate interface (Figure 5.b-d), causing the instability of the right oil-hydrate interface.

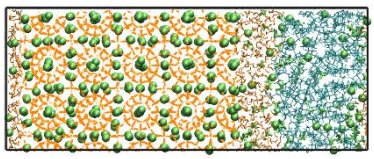

Fig.2. pure model at 200 ns

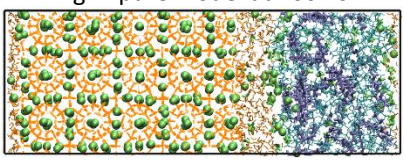

Fig.3. 20-C_{17} model at 200 ns

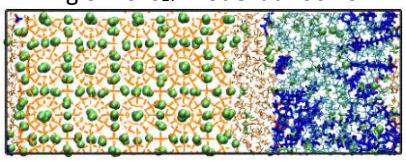

(a) 65 ns

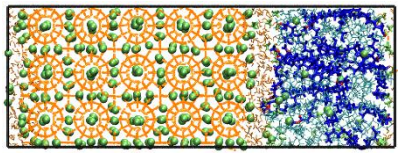

(b) 158 ns

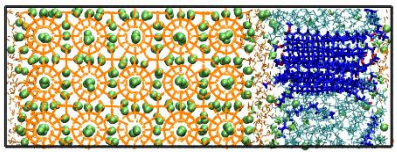

(c) 200 ns

Fig.4. 20-C_{18} model at critical simulation times

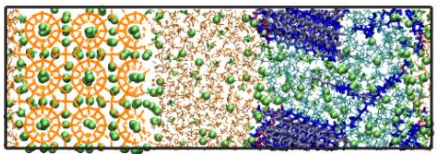

(a) 30 ns

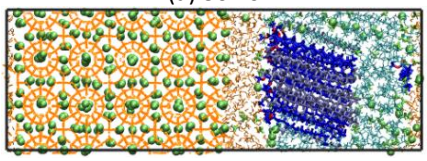

(b) 100 ns

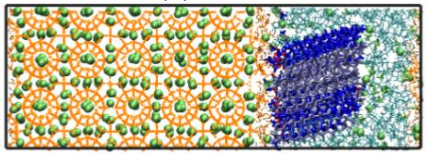

(c) 135 ns

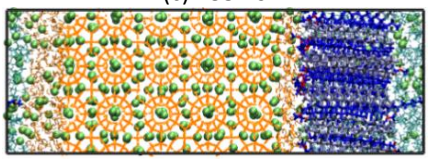

(d) 200 ns

Fig.5. C_{17}-C_{18} model at critical simulation times

3.2 Wax crystallization analysis

The crystallization of wax molecules was observed in 20-C_{18} model after hydrate formation (Figure4.c) and in C_{17}-C_{18} model at the beginning of simulation (Figure5.a). Wax molecules remained dispersed throughout the simulation in 20-C_{17} model (Figure 3). The wax content that governs wax crystallization can be affected by two factors in the simulations, one is the number of wax molecules, and the other is the number of methane molecules in the oil phase. Particularly, the dissolution of methane molecules may increase the distance between the molecules in the oil phase, weaken the van der Waals effects between them, and inhibit the crystallization of wax molecules[18]. As shown in Table 1, the increase in the number of wax molecules and the consumption of methane molecules with the growth of hydrate could significantly increase wax content, contributing to wax crystallization.

Tab.1. Wax content of different models in the first run at critical simulation times

model	20-C_{17}	20-C_{18}	C_{17}-C_{18}
simulation time	200 ns	200 ns	30 ns
wax content	13.452 %	15.607 %	24.354 %

3.3 Potential energy analysis

Potential energy curves that are averaged over the three repeated simulations are shown in Figure 6. The red dotted line represents the equilibrium potential energy, corresponding to the end of bulk hydrate formation and the end of interface hydrate formation, respectively.

Generally, the presence of wax molecules increased the randomness of the hydrate growth process, shown from the error bars in Figure 6. For pure model and 20-C_{17} model, the hydrate growth stage is basically the same, except that 20-C_{17} model exhibits a longer hydrate growth time. For 20-C_{18} model, longer hydrate growth time results in greater amount of hydrate formation, which is consistent with the experimental researches of Chen et al.[7] For C_{17}-C_{18} model, uncertainty exists in the amount of hydrate formation due to the metastability of right oil-hydrate interface. Besides, the 20-C_{18} model has a greater potential energy drop than the C_{17}-C_{18} model during oil-water interface hydrate formation period, which should be ascribed to the crystallization of wax molecules during this period in 20-C_{18} model (Figure 4.b-c).

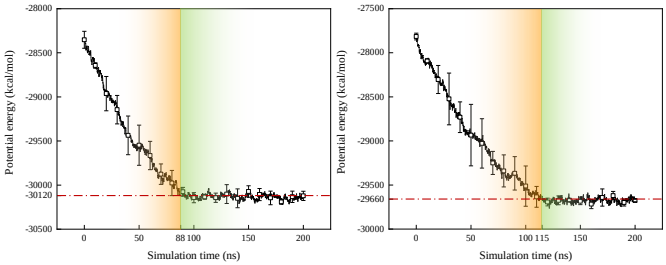

(a) pure model (b) 20-C_{17} model

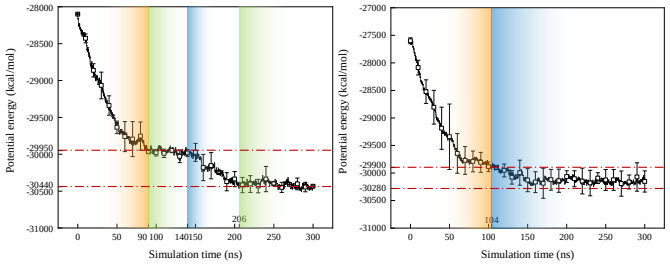

(c) 20-C_{18} model (d) C_{17}-C_{18} model

Fig. 6. Potential energy of four simulation models (orange, bulk hydrate formation period; green, equilibrium period; blue, oil-water interface hydrate formation period)

4. CONCLUSIONS

Nanosecond simulations are performed to study the effect of surface-active/non-surface-active wax molecules on the growth of methane hydrate in the hydrate-water-oil system, and the following conclusions are obtained:

1) The hydrophilic ends of C_{18}s can promote the conversion of the thin water film at the oil hydrate interface into hydrate.

2) The wax crystallization is affected by the number of wax molecules and methane molecules in the oil phase.

3) Addition of non-surface-active wax molecules inhibits hydrate growth, while addition of surface-active wax molecules extends hydrate growth time to achieve a greater amount of hydrate formation.

ACKNOWLEDGEMENT

This work was supported by the Beijing Municipal Natural Science Foundation [No. 3192027]; National Natural Science Foundation of China [No.: 51874323, U20B6005, 52104069]; Science Foundation of China University of Petroleum, Beijing [No.: 2462020YXZZ045, 2462020XKBH012]

REFERENCE

[1] Gao S. Investigation of interactions between gas hydrates and several other flow assurance elements. Energy Fuels 2008;22:3150–3.

[2] Ji H. Thermodynamic modelling of wax and integrated wax-hydrate. thesis. Heriot-Watt University, 2004.

[3] Song G, Li Y, Wang W, et al. Numerical simulation of hydrate slurry flow behavior in oil-water systems based on hydrate agglomeration modelling. J Pet Sci Eng 2018;169:393–404.

[4] Zheng H, Huang Q, Wang W, et al. Induction time of hydrate formation in water-in-oil emulsions. Ind Eng Chem Res 2017;56:8330–9.

[5] Shi B, Chai S, Ding L, et al. An investigation on gas hydrate formation and slurry viscosity in the presence of wax crystals. AIChE J 2018;64:3502–18.

[6] Song X, Xin F, Yan H, et al. Intensification and kinetics of methane hydrate formation under heat removal by phase change of *n* -tetradecane. AIChE J 2015;61:3441–50.

[7] Chen Y, Shi B, Liu Y, et al. Experimental and theoretical investigation of the interaction between hydrate formation and wax precipitation in water-in-oil emulsions. Energy Fuels 2018;32:9081–92.

[8] Liu Y, Shi B, Ding L, et al. Study of hydrate formation in water-in-waxy oil emulsions considering heat transfer and mass transfer. Fuel 2019;244:282–95.

[9] Zi M, Chen D, Wu G. Molecular dynamics simulation of methane hydrate formation on metal surface with oil. Chem Eng Sci 2018;191:253–61.

[10] Liao Q, Shi B, Li S, et al. Molecular dynamics simulation of the effect of wax molecules on methane hydrate formation. Fuel 2021;297:120778.

[11] Binks BP, Rocher A. Effects of temperature on water-in-oil emulsions stabilised solely by wax microparticles. J Colloid Interface Sci 2009;335:94–104.

[12] Horn HW, Swope WC, Pitera JW, et al. Development of an improved four-site water model for biomolecular simulations: TIP4P-Ew. J Chem Phys 2004;120:9665–78.

[13] Jorgensen WL, Maxwell DS, Tirado-Rives J. Development and testing of the OPLS all-atom force field on conformational energetics and properties of organic liquids. J Am Chem Soc 1996;118:11225–36.

[14] Cao Z, Tester JW, Sparks KA, et al. Molecular computations using robust hydrocarbon−water potentials for predicting gas hydrate phase equilibria. J Phys Chem B 2001;105:10950–60.

[15] Neelov A, Holm C. Interlaced P3M algorithm with analytical and ik-differentiation. J Chem Phys 2010;132:234103.

[16] Tung Y, Chen L, Chen Y, et al. The growth of structure I methane hydrate from molecular dynamics simulations. J Phys Chem B 2010;114:10804–13.

[17] Ryckaert J-P, Ciccotti G, Berendsen HJC. Numerical integration of the cartesian equations of motion of a system with constraints: molecular dynamics of n-alkanes. J Comput Phys 1977;23:327–41.

[18] Li B, Liu G, Chen L. Study on the influence mechanism of CH4 dissolution on the intermolecular interaction between crude oil molecules based on molecular dynamics simulation. CIESC J 2021;72:1253–63.